PHYSICAL REVIEW
LETTERS

VOLUME 72 16 MAY 1994 NUMBER 20

Measurement of the Silicon (220) Lattice Spacing

G. Basile, A. Bergamin, G. Cavagnero, and G. Mana
Consiglio Nazionale delle Richerche–Istituto di Metrologia "G. Colonnetti," strada delle Cacce 73, 10135 Torino Italy

E. Vittone
Università di Torino–Dipartimento di Fisica Sperimentale, via P. Giuria 1, 10125 Torino Italy

G. Zosi
Università di Torino–Istituto di Fisica Generale "A. Avogadro," via P. Giuria 1, 10125 Torino Italy
(Received 28 December 1993)

The (220) lattice spacing of a silicon crystal was measured by combined x-ray and optical interferometry to about 3×10^{-8} relative accuracy. The value obtained is $d_{220} = 192\,015.551 \pm 0.005$ fm. After correcting for the impurity-induced lattice contraction, $d_{220} = 192\,015.569 \pm 0.006$ fm is obtained.

PACS numbers: 06.20.Jr, 06.30.Bp, 61.10.Lx, 07.60.Ly

The (220) lattice spacing value of silicon is essential for the highest accuracy measurement of the Avogadro constant, of the de Broglie wavelength of thermal neutrons (for the h/m_n ratio and α determinations), and of x-ray and γ-ray wavelengths. Since Bonse and Hart in 1965 [1] first succeeded in obtaining x-ray interference, it has been clear that combined x-ray and optical interferometry would allow the silicon d_{220} to be measured with unprecedented accuracy [2].

The first d_{220} value was obtained in 1973 by Deslattes at the National Institute for Standards and Technology (NIST) [3]. It was a milestone in linking visible and x-ray wavelengths and pointed the way for all subsequent experiments. In 1981, Becker at the Physikalisch-Technische Bundesanstalt (PTB) obtained a more accurate value [4,5]. Further investigations led to the discovery of an error in the NIST measurement [6] and, in 1988, we reported [7] a preliminary d_{220} value close to that obtained by the PTB group, but with a larger uncertainty. We have refined our previous experiment [8] and investigated influence quantities in more detail. In the new silicon d_{220} value we give here, the error is significantly reduced. In the meantime, Windisch [9] related the silicon d_{220} value to crystal impurities and laid the basis for the extrapolation of an invariant value.

Principle of measurement.—In an ideal measurement, an x-ray and an optical interferometer are so coupled as to have the same base line, along which the measuring crystal is moved. During movement, the intensity of the outgoing beams is modulated and the periods are d_{220} (x-ray) and the half wavelength $\lambda/2$ of the laser beam (optical). The equivalence between the period of x-ray fringes and d_{220} is a delicate point which deserves careful investigation [8,10–12]. What is measured is the ratio n/m of x-ray to optical periods and, since the optical wavelength is stabilized by saturated absorption at the component "e" of the hyperfine transition 11-5 $R(127)$ of the molecule $^{127}I_2$, that is, $\lambda = 632\,991\,194.7 \pm 0.1$ fm, the relation $d_{220} = (m/n)\lambda/2$ gives the absolute spacing.

The resolution of the measured value is limited by the displacement of the measuring crystal; in our experiment it was $270\lambda/2$ (about 85 μm). Starting from the approximation $n(m = 1) = 1648.3$ and by measuring the decimal places of $n(m)$ over increasing displacements, we obtained the approximation $n(m = 100) = 164\,828.1$. The final step was to measure the decimal places of $n(m = 270)$.

Experimental setup.—In addition to the greater displacement, novelties included refined techniques and detailed analysis of interference patterns which allowed bet-

0031-9007/94/72(20)/3133(4)$06.00

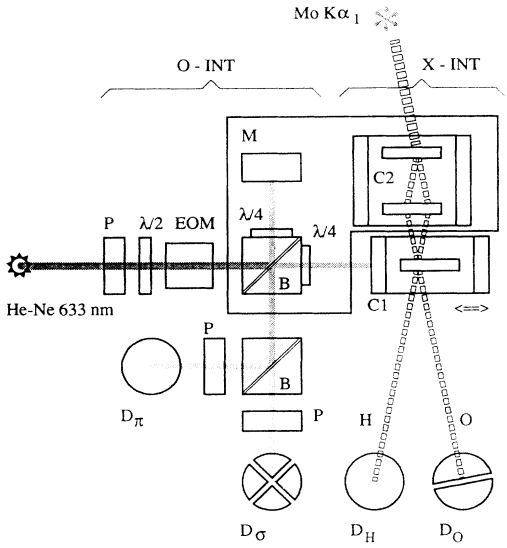

FIG. 1. Schematic drawing of the combined x-ray and optical interferometer. X-INT x-ray interferometer: C1 and C2 movable and fixed crystals, O and H transmitted and diffracted beams, D_O (position-sensitive), and D_H photodetectors. O-INT polarization encoding optical interferometer: B polarizing beam splitters, M fixed mirror, P polarizers, EOM phase modulator, D_σ (position-sensitive), and D_π photodiodes.

ter understanding of influence phenomena. A schematic drawing of the x-ray and optical interferometers is shown in Fig. 1. The x-ray interferometer is formed by two entirely separated crystals with their fronts and backs optically polished and coated to obtain reference mirrors ideally parallel to the (220) lattice planes. The experiment was carried out *in vacuo* (pressure being 0.5 Pa or lower) and the setup was shielded from temperature fluctuations by a thermal enclosure and from seismic noise by an antivibration support. The average count rate and the fringe contrast were 6200 counts/s and 40%, respectively. Fringe subdivision to within $10^{-3}d_{220}$ was obtained by scanning about three fringes and by data fit [13]. Scan velocity was 20 pm/s, sample number 700, counting window 40 ms, and sample duration 28 s.

The laser beam is delivered by a single-mode polarization-preserving fiber ensuring simple and stable remote alignment and positioning of the beam. Improved polarization encoding and phase modulation [14,15] reduced the noise in defining dark fringes and made it possible to achieve prompt movements with picometer resolution and damping of disturbances due to vibrations [16]. The crystal attitude was measured by monitoring phase shifts (differential displacements) between four portions of the interference pattern. Null rotations were measured to within 0.5 nrad and the unbalancing was used to compensate for attitude errors due to parasitic tilts of the translation stage [17–19]. However, errors apt to occur in angle measurements [20] prevented the rotation locking at zero from being better than a few nanoradians. The near perfect alignment necessary to perform simultaneous displacement and angle measurements was much simplified by the use of a simple Michelson geometry and of an auxiliary mirror. Instabilities arising from the use of different origins for x-ray and optical rules were lessened by placing the fixed components of the interferometers on the same (silicon) plate. The running of the experiment proved that the small residual drift (about $10^{-2}d_{220}$ during the 100 s required to cover the $270\lambda/2$ displacement) between the two rules did not affect measurement results: data were easily corrected by averaging the results of scans taken in opposite directions.

TABLE I. Summary of silicon d_{220} determinations.

Laboratory	Reference	Date	Value (fm)
NIST [a,b]	[3]	1973	192 015.902 ± 0.019
PTB [a,b]	[4]	1981	192 015.560 ± 0.012
CODATA [b]	[29]	1986	192 015.540 ± 0.040
IMGC [b,d]	[7]	1988	192 015.524 ± 0.054
PTB [c]	[4,9]	1990	192 015.568 ± 0.012
IMGC [c]	...	1994	192 015.569 ± 0.006

[a]Not corrected for C and O contents.
[b]$t_{68} = 22.500\,^\circ$C, vacuum.
[c]$t_{90} = 22.500\,^\circ$C, vacuum.
[d]Amended for imperfect alignment of the laser beam.

The experiment first exploits information redundance in interference fringes. As shown in Fig. 1, x-ray fringes are observed in transmitted (the top and the bottom parts being detected separately) and diffracted beams. Similarly, optical fringes are observed by projecting output polarization on vertical (the top, bottom, left, and right parts being observed separately) and horizontal linear polarizations which are the phase-modulated normal modes of the input beam. Since each of the pairs of x-ray and optical fringes yields measurement values which respond to different errors, imperfections in the measurement were easily revealed [20,21]. In such a way, an error in the procedure previously adopted for laser beam alignment was discovered and resulted in a $2.3 \times 10^{-7}d_{220}$ bias of our earlier value [7]. The amended value is given in Table I. Finally, the crystal temperature was measured to within 3 mK by using a platinum resistance thermometer, periodically calibrated in accordance with ITS-90.

Results.—The histogram in Fig. 2 groups 196 successive measurement values obtained by moving the measuring crystal between optical orders $m = 0$ and $m = 270$; the standard deviation of single measurements value is 0.8×10^{-8}. Before the silicon d_{220} is calculated, the n/m ratio must be corrected for several effects; Table II shows these corrections and their uncertainties. The overall error has been obtained by adding up each of the contributions in quadrature. The wavelength *in vacuo* of the laser beam was corrected for the refractive index of the residual gas, mostly water vapor. Besides, as a re-

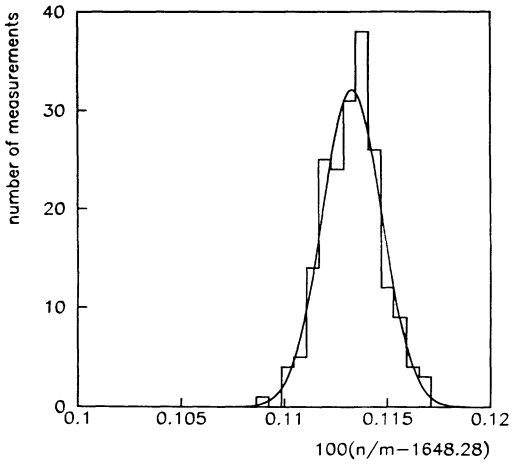

FIG. 2. Frequency distribution of 196 measured values of the n/m ratio. Data were referred to $t_{90} = 22.500\,^{\circ}\mathrm{C}$. The solid line is the distribution of a normal variable having the same mean and standard deviation.

sult of diffraction, the interfering wave fronts bend and the period of optical fringes is different from half the wavelength of a plane wave [20,22]. The alignment error σ_δ of the laser beam biases quadratically the measurement value; the relevant error is a χ^2 variable with $\sigma_\delta^2/2$ mean and $\sigma_\delta^2/\sqrt{2}$ standard deviation. A 0.5 mΩ offset in the measurement of the platinum resistance, which corresponds to a temperature offset of 2 mK, needed correction. Other errors are due to the different projection angles of the crystal movement over the x-ray and optical base lines and to the different movements which are sensed by x-ray and optical interferometers (Abbe's error). Since the crystal moves along a line bisecting the normals to mirror and (220) lattice planes, the projection error is a normal variable having zero mean and standard deviation $\beta\sigma_\alpha$, where σ_α is the bisection error and $\beta = 0.16$ mrad the mirror-to-lattice angle. The attitude error σ_ξ of the active guiding system, combined with the error σ_h of base line overlapping, produces the Abbe's error. It is a random variable having zero mean and standard deviation $\sigma_\xi\sigma_h$. Owing to random effect of chemical etching, the interferometer focusing and the analyzer thickness may be different before and after the movement. These facts cause additional contributions to the number of x-ray fringes covered and the global error has been estimated to be 0.8×10^{-8} [8,10–12]. To increase measurement resolution, the results of measurement repetitions over short periods of time were averaged in order to obtain a single value for the ratio n/m. In a typical half an hour measurement cycle, twenty data are collected and averaged. Reproducibility was investigated by analyzing 92 measurement cycles carried out between May 1st and December 15th, 1993. In the meantime, the experimental setup was partially reassembled a few times. Results are given in Fig. 3. Some of the

TABLE II. Corrections and uncertainties ($\times 10^8$) of d_{220}.

Optical wavelength	-0.2 ± 0.2
Fresnel's diffraction	2.5 ± 0.8
Laser beam alignment	0.3 ± 0.5
Crystal temperature	0.5 ± 0.8
Movement direction	0.0 ± 1.8
Abbe's error	0.0 ± 0.8
Surface roughness	0.0 ± 0.8
Statistic (mean)	0.0 ± 0.5
Overall (IMGC crystal)	3.1 ± 2.5
Crystal impurities	9.3 ± 1.4
Overall (silicon)	12.4 ± 2.9

contributions to the overall error depend, at least partially, upon on-line measurements of influence quantities and upon the actual performances of the feedback loops. The 1.1×10^{-8} standard deviation of a single average estimated from the data in Fig. 3 is therefore consistent with the error analysis carried out. However, since the error correlation is not known, measurement uncertainty is not expected to be reduced by further averaging of the data. The final value of the (220) lattice spacing of the Istituto di Metrologia "G. Collonetti" (IMGC) reference silicon crystal is

$$d_{220} = 192\,015.551 \pm 0.005 \text{ fm}, \quad (1)$$

but $t_{90} = 22.500\,^{\circ}\mathrm{C}$ and *in vacuo*. A summary of the d_{220} values so far available is given in Table I.

The d_{220} determination in specific crystals is not of general interest, since it is related to the binding condition between individual atoms. Values, to be meaningful and comparable, must be referred to the same temperature and pressure and corrected for lattice defects and for crystal impurities and isotopic composition. Our

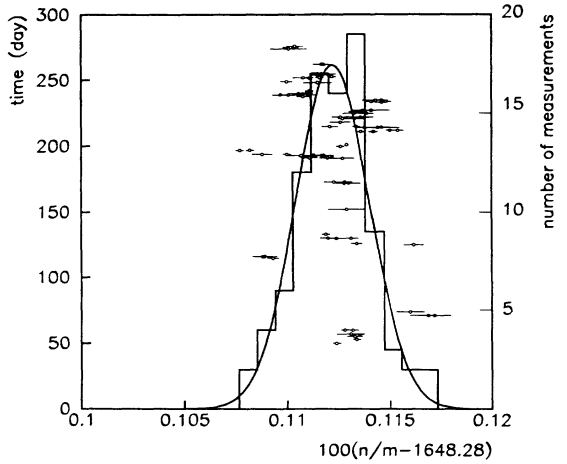

FIG. 3. Averages of data collected in 92 measurement cycles and their frequency distribution. Data were referred to $t_{90} = 22.500\,^{\circ}\mathrm{C}$. The solid line is the distribution of a normal variable having the same mean and standard deviation.

crystal was grown and purified by float-zone melting by MEMC Electronic Materials (formerly Dynamite Nobel Silicon). We have no information about vacancies, vacancy clusters, self-interstitial, and electrically neutral impurities; as regards the isotopic composition recent theoretical [23,24] and experimental [25] investigations show the influence of the different isotope contents of natural crystals to be negligible. Carbon and oxygen are considered the only cause of changes in lattice spacing at the present level of accuracy [9]. Their effects are investigated in Refs. [9,26] which also give the relevant corrections. According to the carbon and oxygen contents of our crystal [27] [$N_C = (1.37 \pm 0.02) \times 10^{16}$ cm^{-3}, $N_O = (4 \pm 1) \times 10^{14}$ cm^{-3}] the impurity-induced lattice contraction is $(9.3 \pm 0.7) \times 10^{-8} d_{220}$. The nonuniform distribution of impurity atoms causes short and long range strains which have been averaged by the integration of the interference pattern and by repeating the d_{220} measurement along the crystal. The global error of the impurities correction has been estimated to be 1.4×10^{-8}. The (220) lattice spacing (at $t_{90} = 22.500\,^{\circ}$C and *in vacuo*) extrapolated to null contents of carbon and oxygen is

$$d_{220} = 192\,015.569 \pm 0.006 \text{ fm}. \quad (2)$$

In Table I, the PTB value [4] is referred to $t_{90} = 22.500\,^{\circ}$C and is corrected for impurities according to the data in [9]; the perfect agreement with the value (2) must be considered fortuitous. Additionally, a comparison between IMGC and PTB samples is in progress at PTB; preliminary results [28] agree with the difference between (1) and the value reported in [4]. As regards the value recommended by the Task Group on Fundamental Constants of the Committee on Data for Science and Technology (CODATA) [29], it has to be noted that it refers to an ideally pure silicon crystal and should be invariant. In fact, the recommended value was a direct outcome of the adjustment and minimized the inconsistency between the values of the Avogadro constant obtained from $N_A = (M/\rho)/\sqrt{8} d_{220}^3$ and from $N_A = c m_e M_p \alpha^2 / 2 m_p h R_\infty$, where the symbols have the usual meanings. The results obtained indicate that the d_{220} values measured in different crystals can be connected better than had previously been assumed and suggest the updating of the recommended value.

Conclusions.—We emphasize that the results reported here are to be examined in connection with the incoming new evaluation of a consistent set of values of the fundamental physical constants and with the determination of N_A and of the h/m_n ratio. In particular, a determination of N_A based on the d_{220} value given here is in progress at IMGC; results will be presented at the 1994 Conference on Precision Electromagnetic Measurements.

Some of the techniques used in this experiment were developed in the framework of a study of combined x-ray and optical interferometry partially supported by the Commission of the European Communities under Contract No. 3422/1/0/182/91/4-BCR-D(30).

[1] U. Bonse and M. Hart, Appl. Phys. Lett. **6**, 155 (1965).
[2] U. Bonse, E. te Kaat, and P. Spieker, in *Precision Measurement and Fundamental Constants*, edited by D.N. Langenberg and B.N. Taylor (Government Printing Office, Washington, DC, 1971), p. 291; I. Curtis *et al. ibid.*, p. 285; R.D. Deslattes, *ibid.*, p. 279.
[3] R.D. Deslattes and A. Henins, Phys. Rev. Lett. **31**, 972 (1973).
[4] P. Becker *et al.*, Phys. Rev. Lett. **46**, 1540 (1981).
[5] P. Becker, P. Seyfried, and H. Siegert, Z. Phys. B **48**, 17 (1982).
[6] R.D. Deslattes, in *The Art of Measurement. Metrology in Fundamental and Applied Physics*, edited by B. Kramer (VCH Publishers, New York, 1988), p. 193.
[7] G. Basile *et al.*, IEEE Trans. Instrum. Meas. **38**, 210 (1989).
[8] G. Basile *et al.*, IEEE Trans. Instrum. Meas. **40**, 98 (1991).
[9] D. Windisch and P. Becker, Phys. Status Solidi A **118**, 379 (1990).
[10] E. Vittone, Ph.D thesis, Politecnico di Torino, 1991.
[11] A. Accotto, E. Vittone, and G. Zosi (to be published).
[12] E. Vittone and G. Zosi (to be published).
[13] A. Bergamin, G. Cavagnero, and G. Mana, Meas. Sci. Technol. **2**, 725 (1991).
[14] G. Basile *et al.*, Metrologia **28**, 455 (1992).
[15] A. Bergamin, G. Cavagnero, and G. Mana, J. Mod. Opt. **39**, 2053 (1992).
[16] A. Bergamin, G. Cavagnero, and G. Mana, Rev. Sci. Instrum. **64**, 168 (1993).
[17] M. Alemanni *et al.*, Metrologia **22**, 55 (1986).
[18] G. Mana, F. Vattaneo, and G. Zosi, Metrologia **26**, 219 (1989).
[19] A. Bergamin, G. Cavagnero, and G. Mana, Rev. Sci. Instrum. **64**, 3076 (1993).
[20] A. Bergamin, G. Cavagnero, and G. Mana (to be published).
[21] A. Bergamin, G. Cavagnero, and G. Mana, Z. Phys. B **76**, 25 (1989).
[22] G. Mana, Metrologia **26**, 87 (1989).
[23] P. Pavone and S. Baroni (to be published).
[24] S. Biernacki (to be published).
[25] P. Becker (private communication).
[26] D. Windisch and P. Becker, Philos. Mag. A **58**, 435 (1988).
[27] B. Pajot, Groupe de Physique des Solides, Universités Paris 7 et Paris 6 (private communication).
[28] P. Becker (private communication).
[29] E.R. Cohen and B.N. Taylor, *The 1986 Adjustment of the Fundamental Physical Constants*, CODATA Bulletin 63 (Pergamon, New York, 1986).

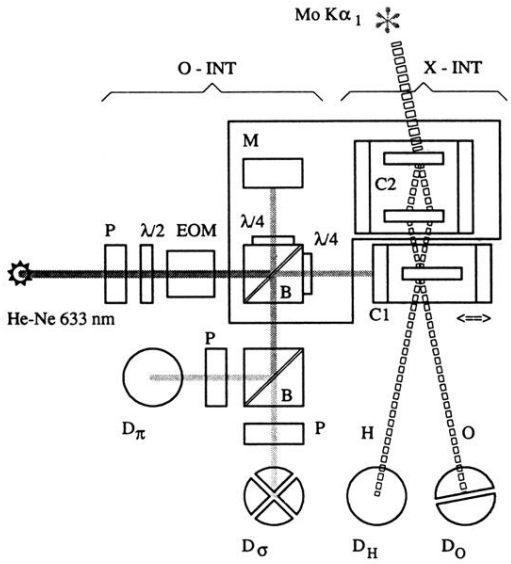

FIG. 1. Schematic drawing of the combined x-ray and optical interferometer. X-INT x-ray interferometer: C1 and C2 movable and fixed crystals, O and H transmitted and diffracted beams, D_O (position-sensitive), and D_H photodetectors. O-INT polarization encoding optical interferometer: B polarizing beam splitters, M fixed mirror, P polarizers, EOM phase modulator, D_σ (position-sensitive), and D_π photodiodes.